International Journal of Innovative Computing, Information and Control
Volume **16**, Number **5**, October **2020**

 ISSN 1349-4198
pp. 1757–1768

FLOW TRACKING OF GLUE SYSTEM BASED ON NON-SINGULAR TERMINAL SLIDING MODE ACTIVE DISTURBANCE REJECTION CONTROL

Jining Guo[1,2], Jun Cao[1,*], Ying Fu[2], Zheng Ma[2], Bingyu Li[2] and Desheng Liu[3]

[1]College of Mechanical and Electrical Engineering
Northeast Forestry University
No. 26, Hexing Road, Xiangfang District, Harbin 150040, P. R. China
Guojining1@163.com; *Corresponding author: zdhcj@126.com

[2]College of Engineering
Bohai University
No. 19, Keji Road, New Songshan District, Jinzhou 121013, P. R. China

[3]College of Information Science and Electronic Technique
Jiamusi University
No. 258, Xuefu Street, Jiamusi 154007, P. R. China
zdhlds@163.com

Received April 2020; revised August 2020

Abstract. *In this study, a control strategy combining active disturbance rejection control (ADRC) with non-singular terminal sliding mode control (NTSMC) is proposed for the uncertainty and external interference of the glue system model. The total disturbance of the system is mainly estimated by the extended state observer in ADRC, and NTSMC is used to compensate the system. The introduction of NTSMC can lead the system to converge in a limited time and can improve the control accuracy of the system. The extended state observer is also effective in eliminating chattering caused by discontinuous control. Through data collection on an experimental platform and MATLAB system identification, the proposed method is analyzed for stability. The proposed ADRC-NTSMC method achieves higher flow tracking accuracy and better active suppression of time-varying disturbances than the nonlinear proportional-integral-derivative method and existing ADRC. The simulation results thus verify the feasibility and effectiveness of the proposed strategy.*

Keywords: Traffic tracking, Extended state observer, Auto disturbance rejection control, Non-singular terminal sliding mode control, Glue system

1. **Introduction.** The amount of glue applied on the surface layer of a particleboard core layer directly affects the static strength, elastic mode, internal binding strength, and other mechanical properties of the plate. It is thus necessary to ensure the stability and uniformity of the application volume, which is of great practical significance for improving product quality and decreasing production costs [1,2]. The glue dosing system for particleboard is characterized by nonlinearity, time lag, and uncertainty [3], and the performance of the system is affected by the uncertainty of the system parameters and various external disturbances, such as fluctuations in power supply, changes in motor speed, the mechanical characteristics of the pump load, and the flow resistance of the line of the viscous fluid. It is thus difficult to establish an accurate mathematical model of a practical system. In addition, the fault-tolerant capability and cost of the entire system

DOI: 10.24507/ijicic.16.05.1757

must also be considered. Due to the demand for the number and accuracy of flow sensors, the cost has significantly increased, as well as the probability of fault [3]. Therefore, it is necessary to introduce a new control strategy for the glue dosing system to improve the system's interference suppression ability and control accuracy.

Traditional proportional-integral-derivative (PID) control has been widely used for the particleboard glue dosing system; however, it is difficult to obtain high dynamic performance because this method requires an accurate mathematical model and is based on the error control method. For the problem of system disturbance suppression, Liu et al. [4] applied the generalized predictive PID control strategy to the glue dosing system. This strategy led to an improved anti-disturbance ability of the system compared to that produced by PID control; however, there remained an error of more than 15% between the actual output and set value of the system.

To solve the interference problem, Sun et al. [5] used neural network predictive control, which has advantages for the nonlinear characteristics of the system model. However, predictive control is a type of model-based control algorithm and cannot solve the problem of system model uncertainty. Using an adaptive sliding mode control algorithm, Liu [3] designed a nonlinear controller to ensure asymptotic stability of the system when the system parameters were perturbed within a certain range. However, no further studies were conducted on the chattering problem caused by high gain.

To ensure effective control, some control strategies [5] assume that all components of the state vector can be measured. However, this is difficult to achieve in actual production. Therefore, estimation of the unobservable state in the control system is necessary. In response to this problem, the extended state observer (ESO) was proposed [6], which is designed to estimate a wide range of disturbances without an accurate model. This method regards the uncertainty of model parameters and unknown interference as the expansion state, which is eliminated by nonlinear feedback (i.e., active disturbance rejection control [ADRC]).

The ADRC method was proposed by Han on the basis of PID control [6]. Its control principle is based on the control target, and it involves a simple algorithm that is independent of an accurate system model and is easy to implement. ADRC has been used in the fields of aerospace engineering, robot control, DC motor control, and power converter circuits [7-10]. However, it has not been reported for glue dosing systems. ADRC can suppress the impact of external disturbance and system uncertainty; however, it is unable to make the system converge quickly. For nonlinear systems, the ability to converge in a limited time is an important dynamic performance indicator.

Sliding mode control is characterized by fast response and high robustness to system parameter changes and external interference. In the late 1980s, the concept of terminal sliding mode control (TSMC) was proposed [11], in which the nonlinear sliding mode replaced the traditional linear sliding mode. This enabled the system state to converge to the equilibrium point in a finite time instead of asymptotically. However, the singular value problem remained in the TSMC, and the chattering phenomenon was still evident due to the existence of the switching function. Therefore, the non-singular terminal sliding mode control (NTSMC) method was proposed [12]. For sliding mode control, the elimination of chattering also eliminates its anti-perturbation capability. Therefore, jitter is the focus of non-singular sliding mode control.

Current anti-chattering methods mainly include the boundary layer design method, approach law method, interference observer method, and other intelligent methods. Each method has its own limitations; for example, the boundary layer method can only ensure that the system state converges to the boundary layer centered on the sliding surface but not to the sliding mode. The reaching law is proposed for the convergence of the initial

state of the system to the sliding surface; the interference observer method is mainly used to eliminate chattering caused by interference. Therefore, case-by-case analysis is required [13-15].

Various scholars have studied a control method combining an ESO and sliding mode control and applied it to various fields. Li and Wang estimated the total disturbance of the system using an ESO and compensated with TSMC. The method was applied to the position tracking problem of an electric cylinder, and improved the tracking accuracy and anti-interference ability of the system [16]. Song et al. improved the generalized state observer by using a switching-type uniformly convergent differentiator to more accurately estimate and attenuate the concentrated perturbation. They derived a multivariable high-order sliding mode feedback law to achieve timed convergence, improving the performance of the traditional ADRC based on the fixed-time high-order sliding mode method [17]. Chen et al. combined ADRC with fast TSMC for robotic lower limb bone tracking control. The simulation results demonstrated that the proposed control strategy and ADRC significantly reduced the chattering of the system [18]. In several methods, the state observer method was used to reduce chattering; however, the designed sliding surface was different.

Based on the aforementioned studies, a new control algorithm is proposed in this paper that combines NTSMC with ADRC to cause the flow tracking to converge to the expected value in finite time. The ESO is designed to treat parameter uncertainty, unmodeled dynamics, and external time-varying perturbations as total disturbances. In addition, fast NTSMC is used to perform effective and accurate compensation to improve the system's disturbance suppression ability. This control has a high speed of convergence and high tracking accuracy.

The remainder of this paper is organized as follows. Section 2 describes the working principle of the system and the system model. Section 3 presents the controller design, while Section 4 presents a simulation of the controller algorithm. The paper is concluded in Section 5.

2. **Mathematical Model of Glue System.**

The gluing control process of the automatic glue dosing control system is described as follows. According to the size of particle flow, the ratio of the particle and glue liquid is set, the sizing pump is controlled to draw the glue liquid from the mixing tank, and the glue liquid is sprayed evenly on the particle through the nozzle. The electromagnetic flowmeter serves as a feedback link to provide the actual flow rate of the glue liquid. After comparison with the set value, the speed of the sizing motor is controlled to glue amount [4].

The open-loop structure of the system with a sensor is illustrated in Figure 1. The squirrel-cage asynchronous motor is powered by a frequency converter, and the speed of the motor can be easily adjusted by changing the frequency of the frequency converter. The flow of the reference point is measured in real time by the flow sensor. An error signal is generated based on the comparison of the given value of the flow with the amount of flow feedback. After processing by the flow regulator, the system produces the appropriate control signal to control the frequency of the frequency converter. In this study, the ESO is used to measure each state output variable and total disturbance. Removing the link of the flow sensor improves the fault tolerance of the system and reduces the cost. To establish a mathematical model of the control objects, each execution unit of the open-loop system is investigated.

2.1. **Frequency converter link.**

The frequency converter uses the constant voltage and frequency ratio control mode. For pump loads, the engineering constant is equivalent to

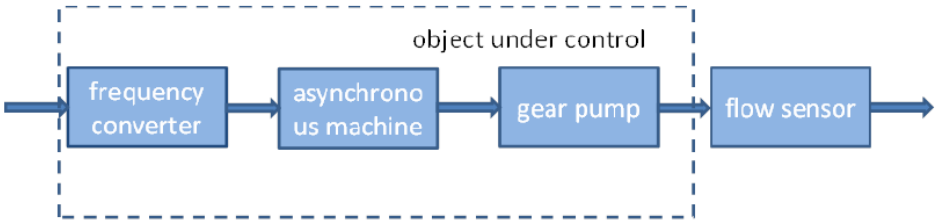

FIGURE 1. Open-loop structure of glue system

an inertial link [19]. Ignoring the simplified low-frequency torque compensation voltage, the mathematical model of the inverter is as follows:

$$U_1 = \frac{K_f f}{T_f s + 1} \tag{1}$$

where U_1 is the motor stator phase voltage, f is the output frequency of the inverter, and K_f is the voltage-frequency conversion coefficient. The value of T_f can be obtained by starting the characteristic curve.

2.2. **Three-phase asynchronous motor link.** If the electromagnetic transient process in the motor is ignored, after simple linearization, the electromagnetic torque T_e of the asynchronous motor is given by the following formula:

$$\begin{aligned} T_e &= \frac{3m_p U_1 (R_2/S)}{\omega_1 \left[\left(R_1 + \frac{R_2}{S} \right)^2 + \omega_1^2 (L_1 + L_2)^2 \right]} \\ S &= 1 - \left(\frac{n_p}{n_0} \right) \end{aligned} \tag{2}$$

where m_p is the magnetic pole pair of asynchronous motors, U_1 is the per-phase voltage of the asynchronous motor stators, ω_1 is the angle speed of the asynchronous motors, R_1 is the stator per phase resistance, R_2 is the rotor-per-phase resistance to the stator side, S is the asynchronous motor transfer rate, n_p is the actual speed of the induction motor, L_1 is the leakage inductance per phase of the stator, and L_2 is the leakage inductance of each phase of the rotor of an asynchronous motor.

The equation of the asynchronous motor mechanical motion is

$$\frac{2\pi}{60} J \frac{dn_p}{dt} = T_e - T_{fz} - \frac{2\pi}{60} B_1 n_p \tag{3}$$

where J is the moment of inertia of the motor, T_{fz} is the load torque, and B_1 is the damping coefficient of the motor shaft.

Here, the load torque of the motor is the input torque of the pump given by the formula

$$T_{fz} = \frac{V \cdot P}{\eta_m} \tag{4}$$

where V is the pump displacement, P is the outlet pressure of the pump, and η_m is the mechanical efficiency of the pump. Therefore, the asynchronous motor approximate linearization transfer function can be calculated as follows:

$$\begin{aligned} &\frac{2\pi}{60} J \frac{dn_p}{dt} = K_1 K_f^2 f - \frac{K_1 K_f^2}{K_2} n_p - \frac{V \cdot P}{\eta_m} - \frac{2\pi}{60} B_1 \eta_p \\ &K_1 = \frac{3m_p}{2\pi R_2}, \; K_2 = \frac{60}{m_p} \end{aligned} \tag{5}$$

After the Laplace transformation, we obtain

$$N(s) = \frac{K_1 K_f F(s) - \frac{V}{\eta_m} P(s)}{\frac{2\pi}{60} J \cdot s + \frac{2\pi}{60} B + \frac{K_1 K_f}{K_2}} \tag{6}$$

The transfer function between speed, frequency, and outlet pressure can be obtained from (6).

2.3. **Gear pump link.** The flow continuity equation for the pump load is given by

$$Q(t) = Q_P(t) - Q_L(t) - Q_C(t) \tag{7}$$

where Q is the total pump output flow (ml/s), Q_P is the theoretical total displacement of the pump (ml/s), Q_L is the leak flow from the pump (ml/s), and Q_C is the loss of flow volume caused by compression (m^3). If the effect of pressure and temperature on the viscosity of the glue is ignored, these values can be calculated as follows:

$$Q_P(t) = \frac{n_p \cdot V}{60} \tag{8}$$

$$Q_L(t) = \frac{C_P}{\mu_T} P_p \tag{9}$$

$$Q_C(t) = \frac{V_0}{\beta_e} \left(\frac{\partial P_p}{\partial t} \right)_{T_0} \tag{10}$$

where C_P is the leak factor of the pump (m^3/s/Pa), P_p is the pressure in the pump (Pa), μ_T is the power viscosity of the glue (N·s/m^2), β_e is the elastic modulus of the glue, and V_0 is the volume of pumps and lines (m^3). Therefore, we can obtain

$$Q(t) = \frac{n_p \cdot V}{60} - \frac{C_P}{\mu_T} P_p - \frac{V_0}{\beta_e} \left(\frac{\partial P_p}{\partial t} \right)_{T_0} \tag{11}$$

According to (11), the relationship amang the total output flow Q of the pump, the actual speed n_p of the induction motor, and the outlet pressure P of the pump can be obtained.

Due to the technical requirements, when the speed of the asynchronous motor changes, the pressure of glue entering the blender or nozzle should be kept as constant as possible. That is, the sizing system should adopt the method of constant pressure supply with frequency conversion. Therefore, outlet pressure P is constant. The transfer function of the entire control object can be described by a second-order system as follows:

$$\begin{aligned} &\frac{Q(s)}{F(s)} = \frac{V K_1 K_f^2}{60 \left(K_3 s + \frac{K_1 K_f^2}{K_2} + K_4 \right) (T_f s + 1)} \\ &K_3 = \frac{2\pi}{60} J,\ K_4 = \frac{2\pi}{60} B \end{aligned} \tag{12}$$

Therefore, the transfer function of the system is given by the final expression:

$$Q(s) = \frac{b_0 F(s)}{a_2 s^2 + a_1 s + a_0} \tag{13}$$

In addition, the system is proved to be stable by the Routh criterion. In practice, the open-loop characteristic of the glue dosing system is a second-order nonlinear uncertain system,

$$\begin{cases} \dot{x}_1 = x_2 = \dot{Q} \\ \dot{x}_2 = f(x_1, x_2) + w(t) + bu \\ y = x_1 \end{cases} \tag{14}$$

where y is the system output, u is the control input of system, x_1 and x_2 are the system state variables, $f(x_1, x_2)$ is the smooth nonlinear function that is bounded and continuously differentiable, $w(t)$ is the system uncertainty and external disturbance, d is the

total disturbance of the system (assuming that it is bounded and has a first derivative), and $d = f(x_1, x_2) + w(t)$.

3. **Composite Controller Design.** ADRC consists of three parts [20], as illustrated in Figure 2: a tracking differentiator (TD), an ESO, and nonlinear state error feedback. The TD can perform the transition process, track the reference input signal $v_0(t)$, and soften the change of $v_0(t)$. The ESO provides an estimated value of the state variables $z_1(t)$, $z_2(t)$ for the object, and $z_3(t)$, the real-time action $d = f(x_1, x_2) + w(t)$ of the system disturbance. The nonlinear state error feedback turns the error between the transition process and the state variable of the object into a nonlinear combination and provides the required control quantity of the object. In this study, the NTSMC method is used for nonlinear state error feedback. Sections 3.1-3.3 introduce the specific design scheme of each link.

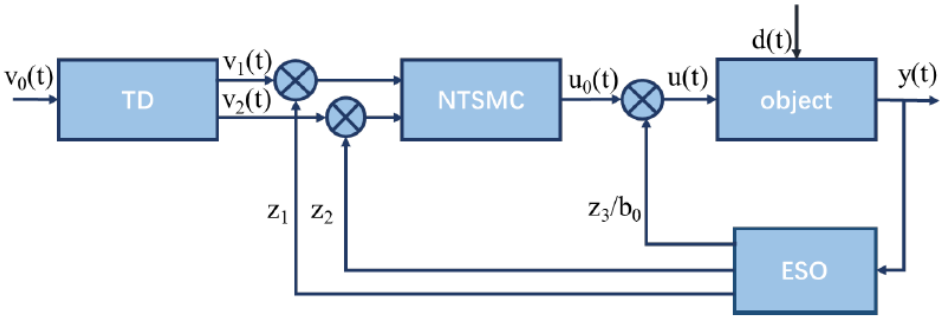

FIGURE 2. Block diagram of non-singular terminal sliding mode control-active disturbance rejection control system

3.1. **Tracking differentiator (TD).** The TD provides the tracking signal and first-order differential signal of the reference instruction signal of the glue dosing system, and can effectively alleviate the overshoot phenomenon caused by the initial error and the discrepancy between the speed and overshoot of the system response.

The discrete form of the TD is given as follows:

$$\begin{cases} e(k) = x_1(k) - v_0(k) \\ x_1(k+1) = x_1(k) + hv_2(k) \\ x_2(k+1) = x_2(k) + hfhan(e(k), x_2(k), r, h_0) \end{cases} \tag{15}$$

where r is the speed factor, h is the sampling period, and h_0 is the filter factor of the instruction signal. The function $fhan(e(k), x_2(k), r, h_0)$ is the fast optimal control synthesis function whose expression is presented in (16). The parameters to be set are r, h, and h_0, which are mainly determined by an empirical trial-and-error method. Generally, $r = 0.0001/h^2$. As a filter factor, the larger the value of h_0, the better the filtering effect. However, a value that is too large leads to tracking lag. Thus, the value is generally $h_0 = 20h$ [20].

$$\begin{cases} d = rh \\ d_0 = hd \\ y = x_1 + hx_2 \\ a_0 = \sqrt{d^2 + 8r|y|} \\ a = \begin{cases} x_2 + \frac{(a_0 - d)}{2} sign(y), & |y| > d_0 \\ x_2 + \frac{y}{h}, & |y| \le d_0 \end{cases} \\ fhan = -\begin{cases} r \cdot sign(a), & |a| > d \\ r\frac{a}{d}, & |a| \le d \end{cases} \end{cases} \tag{16}$$

3.2. **Extended state observer (ESO).** The ESO is the core of ADRC. It can estimate and compensate the total disturbance of the system. Assuming that the total disturbance f of the system is derivable, to simplify the parameter setting, the LESO of the system is constructed as follows:

$$\begin{cases} e_1 = z_1 - y \\ \dot{z}_1 = z_2 - \beta_{01} e_1 \\ \dot{z}_2 = z_3 - \beta_{02} e_1 + bu \\ \dot{z}_3 = -\beta_{03} e_1 \end{cases} \tag{17}$$

where e_1 is the estimate error; z_1, z_2, z_3 are the output of the observer; z_1 and z_2 are the observation value of x_1, x_2, respectively; and z_3 represents the observations of f. The values β_{01}, β_{02}, β_{03} are the gain of the observer. According to the principle of bandwidth, their values should conform to $s^3 + \beta_{01}s^2 + \beta_{02}s + \beta_{03} = (s + \omega_0)^3$. The value ω_0 is the bandwidth of the observer. The relationship between the observer bandwidth and controller bandwidth is in a ratio of 1:3–5 [20].

3.3. **Design of non-singular terminal sliding mode control (NTSMC) law.** To improve the convergence rate of the tracking error and prevent the non-singular problem, fast NTSMC is used to design the error feedback control law. Through the fusion of sliding mode control and ADRC, the parameter setting of the controller is simplified, and the control quality of the system is improved.

There are usually singular problems in traditional sliding mode control; thus, the non-singular terminal sliding mode manifold is adopted to overcome the singular problem [21]:

$$s = \varepsilon_1 + \alpha \varepsilon_2^{\beta} \tag{18}$$

where ε_1 and ε_2 are the systematic error variables, β and α are adjustable parameters, and $\alpha > 0$, $2 > \beta > 1$.

We define glue application error variables as $\varepsilon_1 = Q - Q_d$, where Q_d is the introduction signal (i.e., expected flow). After combining $\varepsilon_2 = \dot{\varepsilon}_1 = \dot{Q} - \dot{Q}_d$, $\dot{\varepsilon}_2 = \ddot{Q} - \ddot{Q}_d$ with (14), we can obtain the error control system of the particleboard glue dosing system as follows:

$$\begin{cases} \dot{\varepsilon}_1 = \dot{Q} - \dot{Q}_d \\ \dot{\varepsilon}_2 = f(x_1, x_2) + w(t) - \ddot{Q}_d + bu \\ y = \varepsilon_1 \end{cases} \tag{19}$$

The time derivative for s is

$$\dot{s} = \varepsilon_1 + \alpha\beta \varepsilon_2^{\beta - 1} \dot{\varepsilon}_2 \tag{20}$$

The general form of the control law is $u = u_{eq} + u_n$, where u_{eq} is the equivalent control term and u_n is the nonlinear control term. Letting $\dot{s} = 0$, we obtain

$$u_{eq} = -\left(\frac{\varepsilon_2^{2-\beta}}{\alpha\beta} + f - \ddot{Q}_d \right) \Big/ b \tag{21}$$

Using the exponential approach law $\dot{s} = -ks - \varepsilon sgn(s)$, we can obtain

$$u_n = (-k_1 s - k_2 sgn(s))/b \tag{22}$$

The control law u is as follows:

$$u = -\left(\frac{\varepsilon_2^{2-\beta}}{\alpha\beta} + f - \ddot{Q}_d + k_1 s + k_2 sgn(s) \right) \Big/ b \tag{23}$$

To reduce chattering, the controller uses saturation and function $sat(s)$ instead of the symbol function $sgn(s)$, and the saturation function is as follows:

$$sat(s) = \begin{cases} 1, & s > \delta \\ \frac{s}{\delta}, & |s| \le \delta \\ -1, & s < -\delta \end{cases} \tag{24}$$

Using the Lyapunov function $V = \frac{1}{2}s^2$ for stability analysis, we obtain

$$\begin{aligned} \dot{V} &= s\dot{s} \\ &= s\left(\varepsilon_2 + \alpha\beta\varepsilon_2^{\beta-1}\dot{\varepsilon}_2\right) \\ &= s\left(\varepsilon_2 + \alpha\beta\varepsilon_2^{\beta-1}\left(f + bu - \ddot{Q}_d\right)\right) \\ &= s\left(\varepsilon_2 + \alpha\beta\varepsilon_2^{\beta-1}\left(-\left(\frac{\varepsilon_2^{2-\beta}}{\alpha\beta} + k_1 s + k_2 sgn(s)\right)\right)\right) \\ &= -\alpha\beta\varepsilon_2^{\beta-1}\left(k_1 s^2 + k_2|s|\right) \end{aligned} \tag{25}$$

When $s \neq 0$ due to $2 > \beta > 1$, we can obtain $\varepsilon_2^{\beta-1} \ge 0$ and $\dot{V} \le 0$. Therefore, points outside the sliding mode manifold can reach the sliding mode manifold in a limited time. In addition, points from any initial state can always converge in a limited time, and the system is globally stable. Thus, the state error feedback control law is designed as follows:

$$\begin{cases} \varepsilon_1 = v_1 - z_1 \\ \varepsilon_2 = v_2 - z_2 \\ u_0 = \dfrac{\varepsilon_2^{2-\beta}}{\alpha\beta} - \ddot{Q}_d + k_1 s + k_2 sgn(s) \\ u = -\dfrac{u_0 + f}{b_0} \end{cases} \tag{26}$$

4. **Simulation Analysis.** On existing equipment in the lab, different frequencies (15 Hz, 25 Hz, 30 Hz, 40 Hz) were selected to measure the output value of the open-loop system flow, as illustrated in Figure 3.

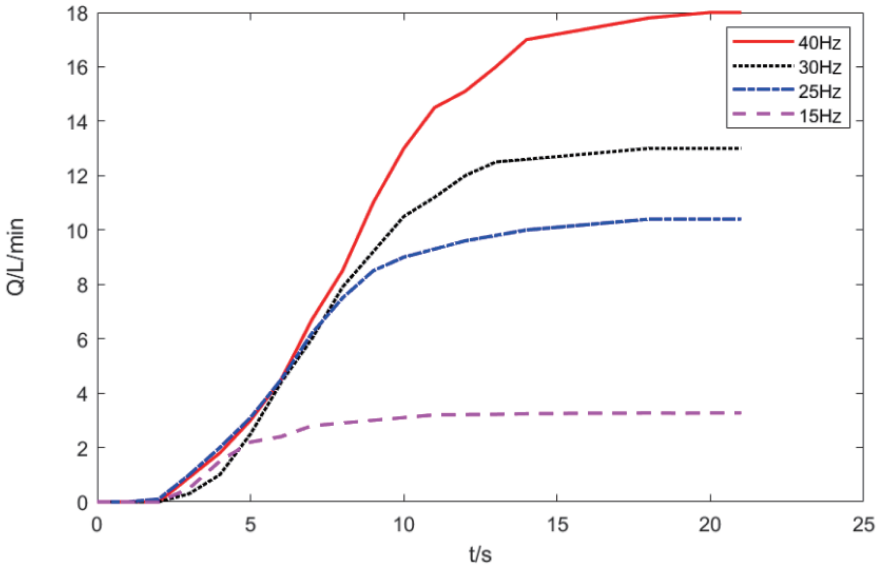

FIGURE 3. Flow output at different input frequencies

Data for the input frequency of 25 Hz were selected to identify the parameters of the control object model. According to (26), the simulation model of the entire control system was established using MATLAB/Simulink. Three methods of nonlinear PD, ADRC, and ADRC-NTSMC were applied to the system, and the model parameters were selected as displayed in Table 1.

TABLE 1. Selection of controller parameters

NPD	ADRC	ADRC-NTSMC
$\delta = 0.02$	$\beta_{01} = 100$	$\beta = 5/3$
$\alpha_1 = 0.75$, $\alpha_2 = 1.5$	$\beta_{02} = 300$	$\alpha = 0.1$
$k_p = 0.5$	$\beta_{03} = 1000$	$k_1 = 450$, $k_2 = 100$
$k_d = 0.1$	$b = 125$	$\delta = 0.05$

The parameters to be set for TD are r and h_0, and the selection method is described in Section 3.1. The parameters to be set in the ESO are β_{01}, β_{02}, and β_{03}, where β_{01} is roughly of the order of magnitude of $\frac{1}{h}$, and the increase in a small range does not have a large influence on the control quality. The selection of β_{02} mainly affects the high-frequency noise of the system, while β_{03} affects the tracking speed of the system. The appropriate value was selected according to the bandwidth and simulation debugging.

When NPD is used for compensation, δ determines the size of the linear interval of the fal function; however, the value of δ cannot be too large or the advantage of nonlinear gain will be lost. Generally, a value of $0.01 < \delta < 0.1$ is appropriate. α_i determines the shape of the fal function. As a rule of thumb, $\alpha_1 = 0.75$ and $\alpha_2 = 1.5$, and k_p and k_d can be adjusted according to bandwidth principle.

In the non-singular terminal sliding mode system, δ is related to the control accuracy of the system. Here, $\delta = 0.05$ was set. For the simulation comparison, a smaller α value indicates a better tracking effect. β is a fraction within the range $(1, 2)$. The numerator and denominator are integers with odd values, which can solve the singular value problem. Larger values of k_1 and k_2 lead to a higher convergence rate; however, they also increase the system jitter.

These methods all used the differential tracker to track and overshoot the input signal. During the nonlinear state error feedback link for the ADRC method, nonlinear PD control was selected. The ESO link of the ADRC-NTSMC method was the same as the parameter setting of the ADRC method. The three control output curves for the input step signal of the system are presented in Figure 4.

There is a disturbance term, $\sin 2\pi t$, in the system model. Figure 4 indicates that nonlinear PD control led the output to reach a stable value; however, there was a small range of fluctuations. Under the same conditions, the ADRC and ADRC-NTSMC methods both stabilized the system output in a short time and improved the anti-disturbance performance of the system. However, ADRC-NTSMC had a shorter adjustment time than ADRC, and there was no overshoot. Therefore, among the three control algorithms, the ADRC-NTSMC method resulted in the best dynamic performance of the system.

Figures 5 and 6 present the output waveforms of the control law u under the ADRC and ADRC-NTSMC algorithms. It can be seen that the chattering phenomenon of the control law output in Figure 6 improves significantly due to the introduction of the observer. Figure 7 presents the curve of the state estimation output (z_1, z_2, z_3) of the ESO and the system output y. The figure reveals that z_1 and y are completely superimposed, which indicates that the ESO can accurately observe the system output value. In addition, it can effectively track the total disturbance $d = -25x_2 + \sin 2\pi t$ of the system. Therefore,

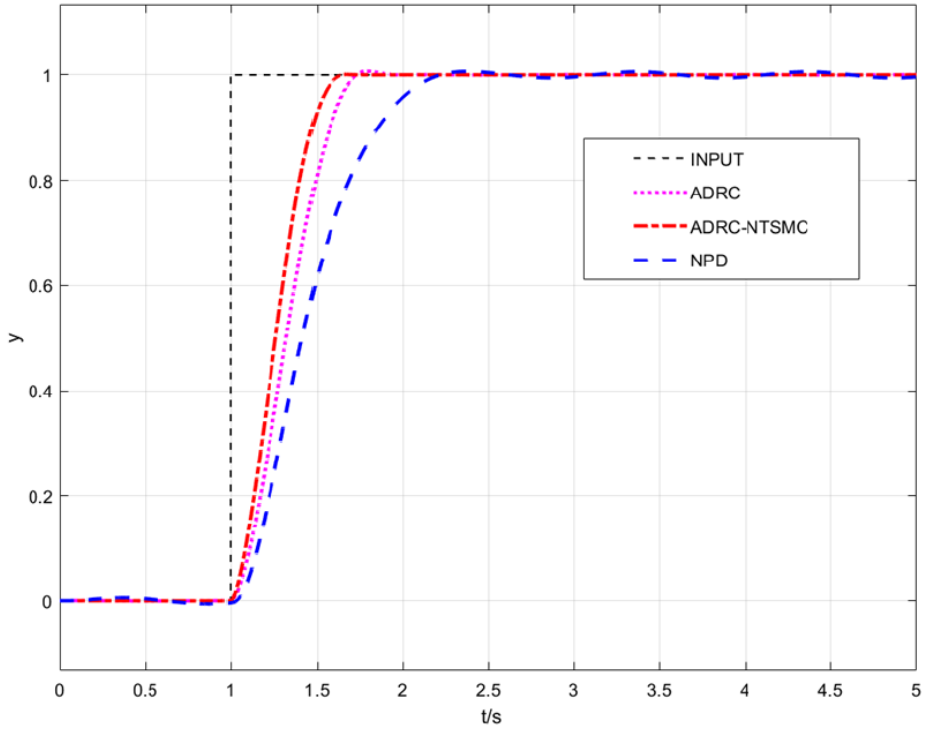

FIGURE 4. Comparison of system output for unit order signal

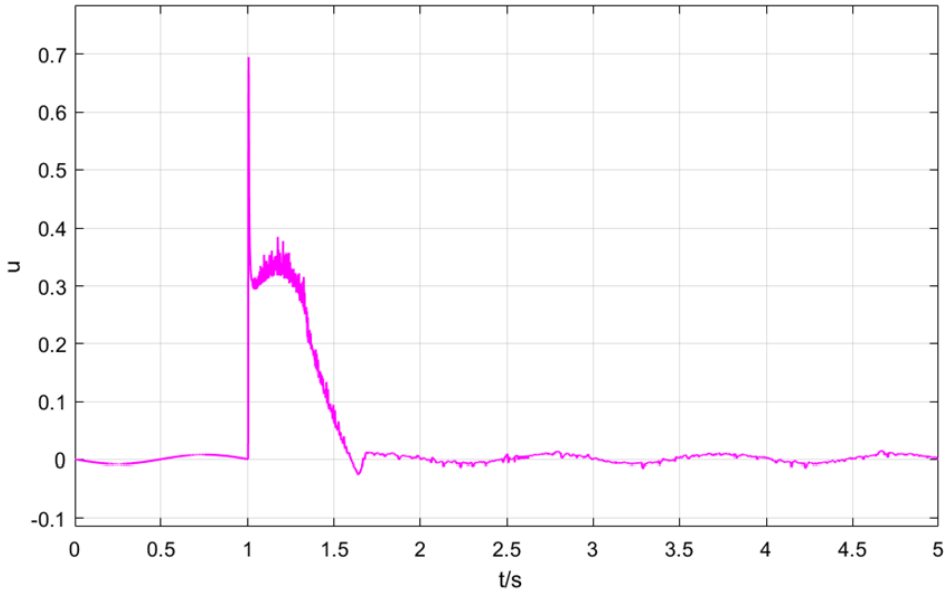

FIGURE 5. Input u value by ADRC method

the ESO can be used for observation and feedback, replacing the flowmeter during the particleboard glue process.

5. **Conclusion.** In this paper, the high-precision flow tracking problem of a particleboard glue dosing system is studied, and the ADRC-NTSMC control strategy is proposed in view of the uncertainty and external interference of the system. This method allows the system output to track the reference input in a limited time and improve the tracking accuracy and anti-disturbance ability of the system. In addition, the introduction of the

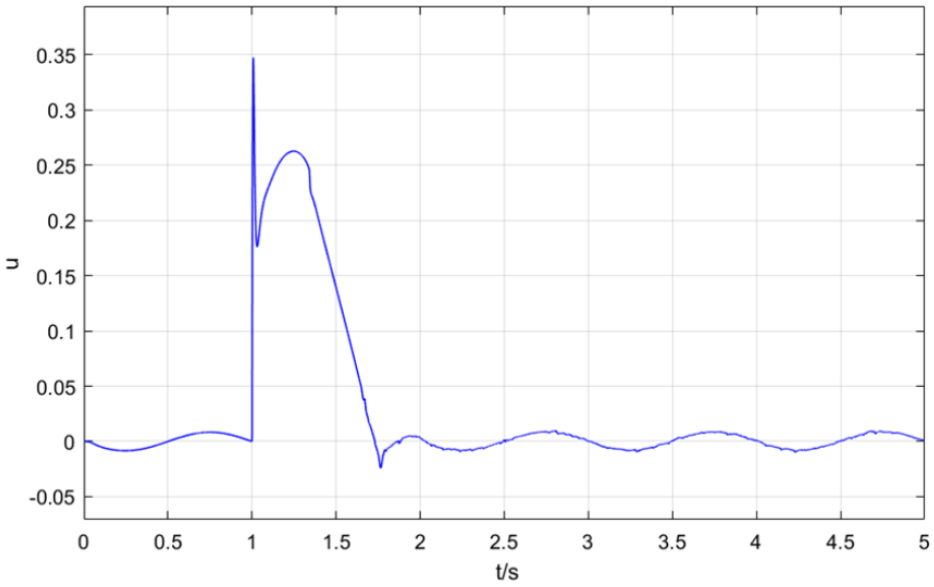

FIGURE 6. Input u value by ADRC-NTSMC method

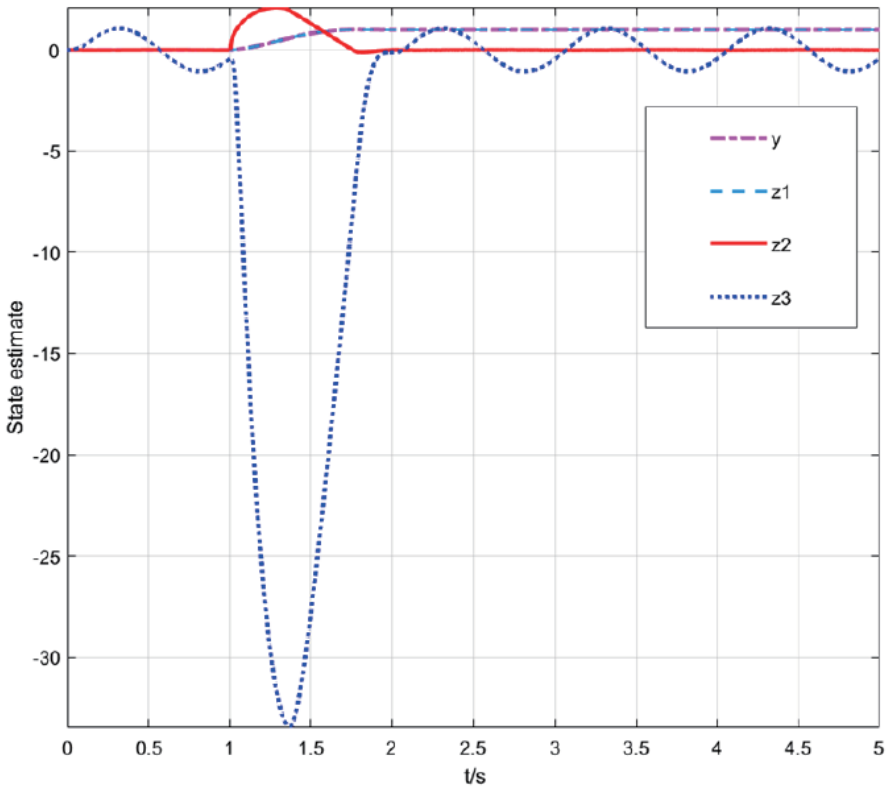

FIGURE 7. Tracking output of ESO

state observer reduces the chattering phenomenon in non-singular sliding mode control. Furthermore, the ESO is designed to effectively track the system state output. Consequently, in the case of sensor failure, the ESO device in ADRC can be used to estimate and detect the system state and total disturbance, thereby improving the fault tolerance of the system and reducing production costs, and has certain practical value for the application of glue dosing system of particleboard.

Acknowledgments. This work was supported in part by the Foundation for Returnees of Heilongjiang Province of China (NO: LC2017027), Jiamusi University Science and Technology Innovation Team Construction Project (CXTDPY-2016-3), Basic Scientific Research Operating Expenses of Heilongjiang Provincial Universities and Colleges for Excellent Innovation Team (2019-KYYWF-1335).

REFERENCES

[1] K. Grzegorz, K. Szymanowski, P. Kozlowski et al., Functional assessment of particleboards made of apple and plum orchard pruning, *Waste & Biomass Valorization*, vol.11, no.6, pp.2877-2886, 2020.

[2] K. Lopatta, K. Böttcher, S. K. Lodhia and S. A. Tideman, Parity codetermination at the board level and labor investment efficiency: Evidence on German listed firms, *Journal of Business Economics*, vol.90, no.1, pp.57-108, 2020.

[3] D. Liu, *Research on Dynamics Characteristic and Robust Control for Glue Dosing of Particleboard*, Ph.D. Thesis, Northeast Forestry University, 2009.

[4] Y. Liu, H. Zhao and D. Liu, Predictive control based on the ration of the particleboard sizing system, *Techniques of Automation & Applications*, vol.28, no.11, pp.26-29, 2009.

[5] L. Sun, J. Cao and Y. Wang, Neural network predictive control of the medium density fiberboard glue system, *Journal of Northeast Forestry University*, vol.42, no.2, pp.136-138, 2014.

[6] J. Han, From PID to active disturbance rejection control, *IEEE Transactions on Industrial Electronics*, vol.56, no.3, pp.900-906, 2009.

[7] X. Shao and H. Wang, Active disturbance rejection based trajectory linearization control for hypersonic reentry vehicle with bounded uncertainties, *ISA Transactions*, vol.54, pp.27-38, 2015.

[8] D. C. Tang, Z. Q. Gao and X. H. Zhang, Design of predictive active disturbance rejection controller for turbidity, *Control Theory & Applications*, vol.34, no.1, pp.101-108, 2017.

[9] J. Yao, Z. Jiao and D. Ma, Adaptive robust control of DC motors with extended state observer, *IEEE Transactions on Industrial Electronics*, vol.61, no.7, pp.3630-3637, 2014.

[10] B. Sun and Z. Gao, A DSP-based active disturbance rejection control design for a 1-kW H-bridge DC-DC power converter, *IEEE Transactions on Industrial Electronics*, vol.52, no.5, pp.1271-1277, 2005.

[11] V. N. Shashihin, Synthesis of control for nonlinear systems, *Automatic Control & Computer Sciences*, vol.53, no.2, pp.97-106, 2019.

[12] X. C. Guo, Z. Y. Liang and C. H. Li, Finite time tracking control of mobile robot based on nonsingular fast terminal sliding mode, *Systems Science & Control Engineering*, vol.6, no.1, pp.492-500, 2018.

[13] J. Yang, S. Li and X. Yu, Sliding-mode control for systems with mismatched uncertainties via a disturbance observer, *IEEE Transactions on Industrial Electronics*, vol.60, no.1, pp.160-169, 2013.

[14] Z. Liu, J. Yu, L. Zhao, Y. Ma, B. Xue and S. Cheng, Adaptive H_∞ sliding mode control for a class of uncertain Markovian jump systems with time-delay, *ICIC Express Letters*, vol.14, no.4, pp.319-327, 2020.

[15] B. Z. Guo, H. C. Zhou, A. S. AL-Fhaid et al., Stabilization of Euler-Bernoulli beam equation with boundary moment control and disturbance by active disturbance rejection control and sliding mode control approaches, *Journal of Dynamical & Control Systems*, vol.20, no.4, pp.539-558, 2014.

[16] D. Li and J. Wang, Nonsingular fast terminal sliding mode control with extended state observer and disturbance compensation for position tracking of electric cylinder, *Mathematical Problems in Engineering*, vol.2018, pp.9808123.1-9808123.12, 2018.

[17] C. Song, C. Wei, F. Yang and N. Cui, High-order sliding mode-based fixed-time active disturbance rejection control for quadrotor attitude system, *Electronics*, vol.7, no.12, 2018.

[18] C. F. Chen, Z. J. Du, L. He et al., Active disturbance rejection with fast terminal sliding mode control for a lower limb exoskeleton in swing phase, *IEEE Access*, vol.7, pp.72343-72357, 2019.

[19] S. Ahmed, H. P. Wang and Y. Tian, Fault tolerant control using fractional-order terminal sliding mode control for robotic manipulators, *Studies in Informatics & Control*, vol.27, no.1, pp.55-64, 2018.

[20] Z. Bingul and O. Karahan, Comparison of PID and FOPID controllers tuned by PSO and ABC algorithms for unstable and integrating systems with time delay, *Optimal Control Applications & Methods*, vol.39, no.4, pp.1431-1450, 2018.

[21] Y. Feng, X. Yu and F. Han, On nonsingular terminal sliding-mode control of nonlinear systems, *Automatica*, vol.49, no.6, pp.1715-1722, 2013.